Journal of Inorganic and General Chemistry
ZAAC
Zeitschrift für anorganische und allgemeine Chemie

DOI: 10.1002/zaac.201600406

ARTICLE

Incorporation of Sulfate or Selenate Groups into Oxotellurates(IV): I. Calcium, Cadmium, and Strontium Compounds

Matthias Weil*[a] and Mahdi Shirkhanlou[a]

Abstract. Seven new mixed oxochalcogenate compounds in the systems $M^{II}/X^{VI}/Te^{IV}/O/(H)$, ($M^{II}$ = Ca, Cd, Sr; X^{VI} = S, Se) were obtained under hydrothermal conditions (210 °C, one week). Crystal structure determinations based on single-crystal X-ray diffraction data revealed the compositions $Ca_3(SeO_4)(TeO_3)_2$, $Ca_3(SeO_4)(Te_3O_8)$, $Cd_3(SeO_4)(Te_3O_8)$, $Cd_3(H_2O)(SO_4)(Te_3O_8)$, $Cd_4(SO_4)(TeO_3)_3$, $Cd_5(SO_4)_2(TeO_3)_2(OH)_2$, and $Sr_3(H_2O)_2(SeO_4)(TeO_3)_2$ for these phases. Peculiar features of the crystal structures of $Ca_3(SeO_4)(TeO_3)_2$, $Ca_3(SeO_4)(Te_3O_8)$, $Cd_3(SeO_4)(Te_3O_8)$, $Cd_3(H_2O)(SO_4)(Te_3O_8)$, and $Sr_3(H_2O)_2(SeO_4)(TeO_3)_2$ are metal-oxotellurate(IV) layers connected by bridging XO_4 tetrahedra and/or by hydrogen-bonding interactions involving hydroxyl or water groups, whereas $Cd_4(SO_4)(TeO_3)_3$ and $Cd_5(SO_4)_2(TeO_3)_2(OH)_2$ crystallize as framework structures. Common to all crystal structures is the stereoactivity of the Te^{IV} electron lone pair for each oxotellurate(IV) unit, pointing either into the inter-layer space, or into channels and cavities in the crystal structures.

Introduction

The peculiar structural feature of oxotellurates(IV)[1] is the $5s^2$ lone electron lone pair situated at the Te^{IV} atom, denoted as *E*. In the majority of cases, *E* is stereochemically active[2] due to its spatial requirement, consequently forming structures with cavities, channels or layers in the neighbourhood of the Te^{IV} atom. In combination with the ability of the Te^{IV} atom to adopt varying coordination numbers from 3 to 5,[3–6] the resulting [TeO_3E], [TeO_4E], or [TeO_5E] building units are also polar. These characteristics can be relevant for the formation of non-centrosymmetric crystal structures or crystal structures with polar directions, features that are indispensable for the existence of interesting physical properties. Whereas pyroelectric, piezoelectric, ferroelectric, or non-linear optical (NLO) properties can principally occur only in crystals with non-centrosymmetric structures, pyroelectric and ferroelectric properties additionally require the condition that the crystal structure must be polar with a non-zero macroscopic dipole moment. As a matter of fact, some of the alkaline earth oxotellurates(IV) phases with composition $MTeO_3$ (M = Ca, Sr) are ferroelectrics,[7–9] and several polymorphs have been structurally determined for each of the $MTeO_3$ phases up to date.[10–16]

In the sense of crystal engineering, the idea behind the current study is a modification of the crystal structures of $MTeO_3$ (M = Ca, Sr, and Cd) compounds by introduction of tetrahedral spacers, i.e. non-centrosymmetric building units into their oxotellurate(IV) frameworks, which may originate in new phases that likewise crystallize in non-centrosymmetric space groups. This approach has already been proven successful for mercury oxotellurates(IV) that were modified with tetrahedral SeO_4 anions, resulting in the two compounds $Hg_3(SeO_4)(TeO_3)_2$ and $Hg_3(SeO_4)(Te_4O_{10})$, both with non-centrosymmetric structures.[17]

For the intended incorporation of SO_4^{2-} or SeO_4^{2-} anions into the oxotellurate(IV) frameworks of calcium, cadmium, and strontium (all with comparable ionic radii as the mercuric ion), we chose hydrothermal methods[18] which bears some advantages over typical solid state reactions using ceramic methods. In comparison with the often harsh reaction conditions required for the latter, e.g. in terms of high temperatures for sufficient diffusion, hydrothermal synthesis usually takes place at much milder conditions and also prevents an oxidation of Te^{IV} by air or an evaporation of compounds volatile at higher temperatures. So far, only a few metal oxotellurate(IV) phases with additional XO_4 groups have been reported, mostly prepared under hydrothermal conditions. This includes the sulfates $Al_2(OH)_2(SO_4)(TeO_3)$,[19] $Fe_2(TeO_3)_2(SO_4)(H_2O)_3$,[20] $Cu_7(OH)_6(TeO_3)_2(SO_4)_2$,[21] $Cu_7TeO_4(SO_4)_5KCl$,[22] the series $RE_2M(TeO_3)_2(SO_4)_2$ (RE = rare earth metal; M = Cu, Co, Zn),[23,24] $Pu(TeO_3)(SO_4)$, $Th(TeO_3)(SO_4)$, $Ce_2(Te_2O_5)(SO_4)_2$,[25] $M_2(TeO_3)(SO_4)H_2O$ (M = Co, Mn),[26] and $BiCu_2(TeO_3)(SO_4)(OH)_3$,[27] and to a much lesser extend the selenates $Sc_2(TeO_3)(SeO_3)(SeO_4)$ (also comprising an oxoselenate(IV) group),[28] $Bi_2(TeO_3)_2(SeO_4)$[29] and the already noted mercury compounds $Hg_3(SeO_4)(TeO_3)_2$ and $Hg_3(SeO_4)(Te_4O_{10})$.[17]

In this communication we report on hydrothermal syntheses and crystal structure determinations of seven new phases in the systems $M^{II}/X^{VI}/Te^{IV}/O/(H)$ (M = Ca, Cd, Sr, and X = S, Se).

Experimental Section

Synthesis: For hydrothermal synthesis of all phases, salts of the corresponding metals were mixed in stoichiometric amounts with TeO_2 and

---

* Prof. Dr. M. Weil
E-Mail: Matthias.Weil@tuwien.ac.at
[a] Institute for Chemical Technologies and Analytics
Division Structural Chemistry
TU Wien
Getreidemarkt 9/164-SC
1060 Vienna, Austria

Table 1. Details of representative experiments for phase formation studies in the systems $M^{II}/X^{VI}/Te^{IV}/O/(H)$ (M = Ca, Cd, Sr; X = Se, S) performed under hydrothermal conditions.

Starting materials; stoichiometric ratios	Phases determined by X-ray powder diffraction of the bulk[a)]	Additional phase(s) determined by single-crystal X-ray diffraction
$CaCl_2·2H_2O/H_2SeO_4/TeO_2/KOH$; 0.215 g / 0.25 mL / 0.152 g / 0.170 g; 3:2:1.5:2	TeO_2,[29] α-$CaTeO_3$,[15] $CaTeO_4$[31]	$Ca_3(SeO_4)(TeO_3)_2$;[b)] $CaTe_3O_8$[32]
$Ca(OH)_2/H_2SeO_4/TeO_2$; 0.117 g / 0.25 mL / 0.165 g; 3:2:1.5	TeO_2, α-$CaTeO_3$, $CaTeO_4$, $CaTe_2O_5$[33]	$Ca_3(SeO_4)(Te_3O_8)$;[b)] $CaTe_2O_5$;[34] $Ca_4Te_5O_{14}$[35]
$CdCl_2/H_2SeO_4/TeO_2/KOH$; 0.217 g / 0.23 mL / 0.113 g / 0.121 g; 3:2:1.7:2	$CdTe_2O_5$,[33] $CdTeO_3$[36]	$Cd_3(SeO_4)(Te_3O_8)$[b)]
$CdSO_4·8/3H_2O/H_6TeO_6/KOH$; 0.30 g, 0.20 g, 0.10 g; 1:1.3:1.5	$Cd(OH)_2$,[37] CdO[38]	$Cd_3(H_2O)(SO_4)(Te_3O_8)$[b)]
$CdCl_2/H_2SO_4/TeO_2/NaOH$; 0.230 g / 0.25 mL / 0.060 g / 0.100 g; 2:2:1:2	TeO_2, $CdTeO_3$, $CdTe_2O_5$, Cd_3TeO_6[39]	$Cd_4(SO_4)(TeO_3)_3$[b)]
$CdO/H_2SO_4/TeO_2/NaOH$; 0.147 g / 0.20 mL / 0.120 g / 0.092 g; 3:2:1.5:2	$CdTe_2O_5$, TeO_2, $CdTeO_3$, CdO	$Cd_5(SO_4)_2(TeO_3)_2(OH)_2$[b)]
$Sr(OH)_2·8H_2O/H_2SeO_4/TeO_2/NaOH$; 0.315 g / 0.26 mL / 0.124 g / 0.100 g; 1.5:2:1:2	$SrTeO_3$,[10] TeO_2, $SrTe_2O_5$[33]	$Sr_3(H_2O)_2(SeO_4)(TeO_3)_2$,[b)] $Sr_5Te_4O_{14}(OH)_2$[40]

a) Main phases appear first, minor phases last in terms of semi-quantitative phase analysis. For all batches additional weak reflections were present that could not be assigned to known phases or the new phases determined by single-crystal X-ray diffraction given in the right column. b) This work.

selenic acid (ca. 80 wt%, prepared by oxidizing SeO_2 in aqueous solution with an H_2O_2/HNO_3 mixture) or sulfuric acid; for some experiments KOH or NaOH were also added to ensure slightly basic conditions. The respective mixture was placed in Teflon containers with ca. 10 mL capacity and filled up with water to about two-thirds of the container volume. After sealing the container with a Teflon lid and placement in a steel autoclave, the mixture was heated at 210 °C for one week. The autoclave was then cooled to room temperature overnight. The solid products were filtered off, washed subsequently with mother liquor, water, and ethanol. All reaction batches consisted of phase-mixtures when inspected optically under a polarising microscope. These findings were confirmed by subsequent powder X-ray diffraction studies of the bulk products. Representative results of the hydrothermal experiments, together with determined reaction products, are gathered in Table 1.

Powder X-ray Diffraction: Samples of the bulk material were ground, fixed with small amounts of petroleum jelly on silicon wafers and measured with Cu-$K_{\alpha1,2}$ radiation in Bragg-Brentano geometry on a PanAlytical X'PertPro system.

Single Crystal Diffraction: For each batch, crystals of good optical quality showing sharp extinctions when imaged between crossed polarizers were pre-selected and were embedded in perfluorinated polyether and fixed on thin silica glass fibres or MiTeGen MicroLoops™. Diffraction data were recorded at room temperature or at 100 K using Mo-K_α radiation either with a Siemens SMART CCD (ω-scans) or a Bruker APEX-II diffractometer (ω- and φ-scans),[41] resulting in data sets of the complete reciprocal spheres. After integration of the data with the program SAINT,[41] an absorption correction based on the semi-empirical "multi-scan" approach was performed with SADABS[41] for all measurements; for the data set of $Cd_3(H_2O)(SeO_4)$-(Te_3O_8) TWINABS[41] was used (see below). All crystal structures were solved by direct methods and were refined using the SHELXTL program package.[42]

Inspection of the diffraction pattern of $Cd_3(H_2O)(SeO_4)(Te_3O_8)$ with the program RLATT[41] revealed two distinct domains with one twin domain rotated by 180° about the reciprocal c^* axis relative to the other twin domain. Reflections belonging to the two domains were separated and further processed in a HKLF5-type reflection file, for which the reflections were merged according to point group $\bar{1}$. This resulted in the following intensity statistics: Mean $I/\sigma = 2.7$ for domain 1 only; mean $I/\sigma = 3.5$ for domain 2 only; mean $I/\sigma = 5.2$ for reflections belonging to both domains. The refined ratio of the two twin domains was 0.6:0.4. Two O atoms of the sulfate group (O12, O13) and one O atom of the cadmium oxotellurate(IV) layer (O11) in this structure were modelled as equally disordered over two sets of sites, denoted as A and B. Since some of the O atoms showed a physically meaningless behaviour when refined anisotropically, all O atoms were refined with a common isotropic displacement parameter; hydrogen atoms of the water molecule present in this structure could not be located from difference maps and thus were excluded from the model but were considered in the formula.

$Cd_3(SeO_4)(Te_3O_8)$, crystallizing in space group $Cmc2_1$, was refined as an inversion twin with a ratio of 0.52:0.48 for the two twin components. For the crystal structure model of $Sr_3(H_2O)_2(SeO_4)$-$(TeO_3)_2$ hydrogen atoms of the water molecules could likewise not be determined reliably and consequently were excluded, but are part of the formula. The position of the OH hydrogen atom in the structure of $Cd_5(SO_4)_2(TeO_3)_2(OH)_2$ was clearly discernible from a difference Fourier synthesis and was refined freely.

The remaining electron density peaks for all structure models were unobstrusive. Numerical data of the data collections and structure refinements are detailed in Table 2 and Table 3. Selected bond lengths and angles are collated in Table 4 and Table 5, together with results of bond valence sums (BVS) calculations[43] for which bond valence parameters of *Brese* and *O'Keeffe*[44] or *Brown*[43] were used.

Table 2. Details of data collections and structure refinements.

	$Ca_3(SeO_4)(TeO_3)_2$	$Ca_3(SeO_4)(Te_3O_8)$	$Cd_3(SeO_4)(Te_3O_8)$
Formula sum	$Ca_3O_{10}SeTe_2$	$Ca_3O_{12}SeTe_3$	$Cd_3O_{12}SeTe_3$
M_R	614.40	774.00	990.96
Crystal size /mm^3	$0.02 \times 0.02 \times 0.36$	$0.04 \times 0.04 \times 0.12$	$0.01 \times 0.02 \times 0.24$
Temperature /°C	23		
Radiation; λ /Å	Mo-K_α; 0.71073		
Diffractometer	Siemens SMART	Siemens SMART	Siemens SMART
Crystal colour; form	colourless, needle	colourless, lath	colourless, needle
Space group (no.)	$P2_1$ (4)	$P2_1/n$	$Cmc2_1$
Formula units Z	2	4	8
a /Å	8.3616(10)	6.9498(12)	18.3402(8)
b /Å	5.6075(7)	9.5789(17)	6.6723(3)
c /Å	11.1853(13)	17.483(3)	18.4360(8)
β /°	108.611(2)	94.469(3)	
V /Å^3	497.03(10)	1160.3(4)	2256.04(17)
μ /mm^{-1}	11.116	12.014	16.496
X-ray density /g·cm^{-3}	4.105	4.431	5.835
Range $\theta_{min} - \theta_{max}$	3.51–32.51	2.34–29.00	2.21–30.49
Range	$-12 \leq h \leq 12$ $-8 \leq k \leq 8$ $-16 \leq l \leq 16$	$-9 \leq h \leq 9$ $-13 \leq k \leq 13$ $-23 \leq l \leq 23$	$-26 \leq h \leq 26$ $-9 \leq k \leq 9$ $-26 \leq l \leq 26$
Measured reflections	8181	14953	16572
Independent reflections	3313	3083	3539
Obs. reflections [$I > 2\sigma(I)$]	3125	2254	3311
R_i	0.0299	0.0876	0.0428
Absorption correction	SADABS	SADABS	SADABS
Trans. coeff. T_{min}; T_{max}	0.673; 0.851	0.327; 0.645	0.110; 0.827
Number of parameters	146	172	183
Ext. coeff. (SHELXL97)	–	–	–
Flack parameter	0.08(3)	–	0.477(13)
Diff. elec. dens. max;min /e$^-$·Å^{-3} (dist. /Å, atom)	2.16 [0.77, Te1]; –1.24 [0.64, Ca3]	4.91 [0.87, Ca3]; –2.04 [1.10, O7]	1.41 [0.79, Te3]; –1.20 [1.17, O13]
$R[F^2 > 2\sigma(F^2)]$	0.0432	0.0483	0.0251
$wR_2(F^2$ all)	0.0944	0.1079	0.0557
GooF	1.097	1.055	1.047

Drawings of structural details were produced using the program ATOMS.[45]

Further details of the crystal structures investigations may be obtained from the Fachinformationszentrum Karlsruhe, 76344 Eggenstein-Leopoldshafen, Germany (Fax: +49-7247-808-666; E-Mail: crysdata@fiz-karlsruhe.de, https://www.fiz-karlsruhe.de/en/leistungen/kristallographie/kristallstrukturdepot/order-form-request-for-deposited-data.html) on quoting the depository numbers CSD-432124 [$Ca_3(SeO_4)(TeO_3)_2$], CSD-432125 [$Ca_3(SeO_4)(Te_3O_8)$], CSD-432126 [$Cd_3(SeO_4)(Te_3O_8)$], CSD-432127 [$Cd_3(H_2O)(SO_4)(Te_3O_8)$], CSD-432128 [$Cd_4(SO_4)(TeO_3)_3$], CSD-432129 [$Cd_5(SO_4)_2(TeO_3)_2(OH)_2$], and CSD-432130 [$Sr_3(H_2O)_2(SeO_4)(TeO_3)_2$].

Results and Discussion

Formation

A notable disadvantage of hydrothermal methods in comparison with ceramic methods is the high(er) number of adjustable parameters, i.e. pressure, concentration, temperature, time, filling degree, used solvent, container material etc. This might be the reason why a prediction of hydrothermally obtained reaction products is usually very difficult (or nearly impossible). In addition, the formation of single-phase products resulting from a hydrothermal reaction is a rather rare phenomenon and usually requires a long-lasting optimization of dependable reaction parameters, in particular for multi-phase systems with different solubility products or redox potentials of individual salts and components, respectively, which were used as starting materials or can form during the reaction. Such difficulties were also observed for hydrothermal reactions in the $M^{II}/X^{VI}/Te^{IV}/O/(H)$ (M = Ca, Cd, Sr and X = S, Se) systems. None of the batches resulted in the formation of a single-phase product (Table 1). Also if some of the hydrothermal reactions were subsequently repeated, then taking into account the exact stoichiometric ratio with respect to the composition of the new phases determined by single crystal diffraction, multi-phase formation prevailed. In all cases the overall amount of incorporated sulfate or selenate in the solid reaction products was much less than nominal present in the reaction mixture.

In this regard, compounds containing tellurium *and* sulfur/selenium were minority products, whereas compounds containing tellurium as the only chalcogen were majority products. As a general trend, formation of Te- *and* S/Se-containing phases becomes more successful at increasing pH values, i.e. at slightly basic conditions. However, under these conditions a reduction of tellurium(VI), employed in the form of telluric acid, to tellurium(IV) can also take place as was the case for the crystallization of $Cd_3(H_2O)(SeO_4)(Te_3O_8)$. On the other hand, an oxidation of the employed tellurium(IV) to tel-

Table 3. Details of data collections and structure refinements.

	$Cd_3(H_2O)(SO_4)(Te_3O_8)$	$Cd_4(SO_4)(TeO_3)_3$	$Cd_5(SO_4)_2(TeO_3)_2(OH)_2$	$Sr_3(H_2O)_2(SeO_4)(TeO_3)_2$
Formula sum	$Cd_3H_2O_{13}STe_3$	$Cd_4O_{13}STe_3$	$Cd_5H_2O_{16}S_2Te_2$	$H_4O_{12}SeSr_3Te_2$
M_R	962.08	1072.46	1139.34	793.05
Crystal size /mm^3	0.01 × 0.06 × 0.10	0.02 × 0.02 × 0.20	0.04 × 0.06 × 0.08	0.06 × 0.13 × 0.09
Temperature /°C	–173	–173	23	23
Radiation; λ /Å	Mo-K_α; 0.71073			
Diffractometer	Bruker APEX-II	Bruker APEX-II	Bruker APEX-II	Bruker APEX-II
Crystal colour; form	colourless, plate	colourless, needle	colourless, block	colourless, fragment
Space group (no.)	$P\bar{1}$ (2)	$P\bar{1}$ (2)	$P\bar{1}$ (2)	$P\bar{1}$ (2)
Formula units Z	2	2	1	4
a /Å	6.7533(8)	5.4219(2)	5.4227(1)	9.7831(16)
b /Å	9.3520(11)	9.9545(3)	8.4179(2)	11.781(2)
c /Å	9.4696(11)	11.6232(3)	8.5154(2)	11.874(2)
α /°	88.719(4)	89.1579(16)	69.2258(8)	90.23(8)
β /°	70.134(4)	87.9578(17)	82.8241(8)	106.578(9)
γ /°	89.634(4)	74.7552(16)	79.1830(9)	103.783(8)
V /Å^3	562.34(11)	604.86(3)	356.258(14)	1270.1(4)
μ /mm^{-1}	13.506	14.269	11.735	19.974
X-ray density /g·cm^{-3}	5.682	5.888	5.311	4.147
Range $\theta_{min} - \theta_{max}$	2.18–29.00	2.74–40.05	2.56–39.19	1.79–36.70
Range	$-8 \le h \le 9$	$-9 \le h \le 9$	$-9 \le h \le 9$	$-16 \le h \le 16$
	$-12 \le k \le 12$	$-18 \le k \le 18$	$-14 \le k \le 14$	$-19 \le k \le 19$
	$0 \le l \le 12$	$-21 \le l \le 21$	$-15 \le l \le 15$	$-19 \le l \le 19$
Measured reflections	2991	57924	36923	75826
Independent reflections	2991	7634	4172	12384
Obs. reflections [$I > 2\sigma(I)$]	2405	6423	3773	8496
R_i	–	0.0583	0.0336	0.0966
Absorption correction	TWINABS	SADABS	SADABS	SADABS
Trans. coeff. T_{min}; T_{max}	0.299; 0.435	0.495; 0.748	0.559; 0.748	0.410; 0.747
Number of parameters	114	194	120	325
Ext. coeff. (SHELXL97)	–	–	0.00568(12)	–
Diff. elec. dens. max;min /e$^-$·Å^{-3} (dist. /Å, atom)	4.18 [0.16, O12B]; –4.78 [0.09, O10]	2.30 [0.71, Cd4]; –2.95 [0.40, Te2]	1.04 [1.39, Te1]; –0.83 [0.81, Te1]	4.92 [0.46, Se1]; –2.17 [0.56, Te4]
R [$F^2 > 2\sigma(F^2)$]	0.0504	0.0274	0.0148	0.0508
wR_2 (F^2 all)	0.1214	0.0437	0.0281	0.1075
GooF	1.073	1.044	1.041	1.049

lurium(VI) can also occur, in this case associated with the formation of the oxotellurates(VI) $CdTeO_4$, $CaTeO_4$, or mixed-valent $CaTe_3O_8$.

Crystal Structures

$Ca_3(SeO_4)(TeO_3)_2$

The crystal structure of $Ca_3(SeO_4)(TeO_3)_2$ is polar (space group $P2_1$). It contains three Ca^{2+} cations, two of which (Ca1, Ca2) are in a distorted octahedral coordination environment by oxygen atoms and one (Ca3) in a distorted bicapped octahedral coordination mode. Cations Ca2 and Ca3 are located at $x \approx 0$; together with the surrounding oxygen atoms, a metal-oxygen layer is formed parallel to (100) through edge- and corner-sharing of the coordination polyhedra. The third Ca^{2+} cation (Ca1) sits in an alternating fashion above and below the layer, thereby bridging one $Ca2O_6$ and three $Ca3O_8$ polyhedra by sharing common edges. Adjacent layers are linked by SeO_4 tetrahedra along [100] into a three-dimensional framework structure encapsulating channels propagating along [010]. The two independent Te^{IV} atoms are located at the outer array of these channels, each capping three oxygen atoms in the shape of a trigonal pyramid, and with the electron lone pair pointing away from the calcium-oxygen layer into the free space of the channels. The two TeO_3 units are isolated from each other and are not linked to the SeO_4 tetrahedron. The crystal structure of $Ca_3(SeO_4)(TeO_3)_2$ is displayed in Figure 1. It exemplifies a rare case of isotypism with a mercury(II) analogue with its peculiar crystal chemistry,[46] another example being the pair $CaAs_2O_6$[47] and $HgAs_2O_6$.[48] Although $Hg_3(SeO_4)(TeO_3)_2$ has been determined with the enantiomorph being present in the crystal structure,[17] a comparison of the two standardized structures with the *compstru* program at the Bilbao Crystallographic server[49] revealed a measure of similarity[50] of $\Delta = 0.11$, that clearly points to the close relation of the two structures. The degree of lattice distortion (S) for the two structures is 0.0102, and the maximal displacement between the atomic positions of a related pair of atoms is in this case 0.64 Å for the pair O10; the arithmetic mean of the distances between two related pairs is 0.307 Å for the two isotypic structures.

$Ca_3(SeO_4)(Te_3O_8)$ and $Cd_3(SeO_4)(Te_3O_8)$

The two compounds have the same formula type and show similar structural features but are not isotypic or related in the sense of a group-subgroup relationship. Both crystal structures (Figure 2 and Figure 3) are composed of three metal-oxygen polyhedra CdO_6 (Cd1), CdO_7 (Cd2, Cd3) and CaO_7

Table 4. Selected interatomic distances /Å, angles /°, and bond valence sums /v.u.[a)]

Ca$_3$(SeO$_4$)(TeO$_3$)$_2$			
Ca1	–	O2	2.225(7)
Ca1	–	O4	2.232(7)
Ca1	–	O9	2.345(8)
Ca1	–	O8	2.443(7)
Ca1	–	O1	2.499(7)
Ca1	–	O3	2.532(7)
Ca2	–	O5	2.256(6)
Ca2	–	O6	2.264(7)
Ca2	–	O3	2.351(7)
Ca2	–	O5	2.377(7)
Ca2	–	O10	2.456(8)
Ca2	–	O4	2.528(7)
Ca3	–	O1	2.393(6)
Ca3	–	O7	2.434(7)
Ca3	–	O6	2.439(7)
Ca3	–	O1	2.442(7)
Ca3	–	O3	2.573(7)
Ca3	–	O2	2.604(8)
Ca3	–	O4	2.633(8)
Ca3	–	O2	2.715(7)
Se1	–	O6	1.625(7)
Se1	–	O3	1.628(7)
Se1	–	O7	1.640(7)
Se1	–	O8	1.641(7)
Te1	–	O5	1.840(6)
Te1	–	O3	1.855(6)
Te1	–	O4	1.858(7)
Te2	–	O6	1.846(6)
Te2	–	O2	1.861(7)
Te2	–	O1	1.875(6)

Ca1 2.08; Ca2 2.07; Ca3 1.83; Se1 6.07; Te1 4.22; Te2 4.11; O1 (Te, 3Ca) 2.15; O2 (Te, 2Ca) 2.24; O3 (Se, Ca) 1.81; O4 (Te, 3 Ca) 2.16; O5 (Te, 2 Ca) 2.15; O6 (Se, Ca) 1.84; O7 (Se, Ca) 1.77; O8 (Se, Ca) 1.85; O9 (Te, 3Ca) 2.18; O10 (Te, 3Ca) 2.25

Ca$_3$(SeO$_4$)(Te$_3$O$_8$)			
Ca1	–	O5	2.314(7)
Ca1	–	O6	2.347(8)
Ca1	–	O7	2.422(7)
Ca1	–	O2	2.435(7)
Ca1	–	O2	2.452(7)
Ca1	–	O4	2.463(7)
Ca1	–	O1	2.535(8)
Ca2	–	O1	2.304(7)
Ca2	–	O2	2.313(7)
Ca2	–	O3	2.364(7)
Ca2	–	O4	2.369(7)
Ca2	–	O10	2.424(9)
Ca2	–	O4	2.505(8)
Ca2	–	O9	2.655(9)
Ca3	–	O9	2.290(8)
Ca3	–	O8	2.388(8)
Ca3	–	O3	2.456(8)
Ca3	–	O3	2.516(8)
Ca3	–	O1	2.534(7)
Ca3	–	O11	2.541(9)
Ca3	–	O5	2.651(8)
Ca3	–	O5	2.860(8)
Se1	–	O11	1.623(8)
Se1	–	O12	1.624(9)
Se1	–	O10	1.628(8)
Se1	–	O6	1.639(8)
Te1	–	O2	1.861(7)
Te1	–	O1	1.866(6)
Te1	–	O8	2.109(7)
Te1	–	O7	2.158(7)
Te2	–	O9	1.826(8)
Te2	–	O4	1.855(7)
Te2	–	O7	1.901(7)
Te3	–	O5	1.847(7)
Te3	–	O3	1.856(7)
Te3	–	O8	1.883(8)

Ca1 2.07; Ca2 2.15; Ca3 1.91; Se1 6.16; Te1 4.04; Te2 4.12; Te3 4.10; O1 (Te, 3Ca) 2.18; O2 (Te, 3Ca) 2.31; O3 (Te, 3Ca) 2.24; O4 (Te, 3Ca) 2.22; O5 (Te, 3Ca) 2.06; O6 (Se, Ca) 1.86; O7 (2Te, Ca) 2.13; O8 (2Te, Ca) 2.31; O9 (Te, 2 Ca) 2.08; O10 (Se, Ca) 1.83; O11 (Se, Ca) 1.77; O12 (Se) 1.56

Cd$_3$(SeO$_4$)(Te$_3$O$_8$)			
Cd1	–	O6	2.213(5)
Cd1	–	O2	2.305(4)
Cd1	–	O7	2.306(4)
Cd1	–	O7	2.320(4)
Cd1	–	O4	2.334(5)
Cd1	–	O10	2.478(5)
Cd2	–	O4	2.221(4)
Cd2	–	O8	2.222(4)
Cd2	–	O5	2.282(4)
Cd2	–	O7	2.399(5)
Cd2	–	O8	2.407(5)
Cd2	–	O1	2.442(5)
Cd2	–	O4	2.530(5)
Cd3	–	O3	2.265(5)
Cd3	–	O6	2.331(5)
Cd3	–	O9	2.333(5)
Cd3	–	O8	2.382(5)
Cd3	–	O5	2.435(5)
Cd3	–	O5	2.460(4)
Se1	–	O11	1.610(7)
Se1	–	O13	1.646(6)
Se1	–	O10	1.650(4) 2x
Se1	–	O14	1.610(8)
Se2	–	O12	1.631(7)
Se2	–	O1	1.635(5) 2x
Te1	–	O5	1.860(5)
Te1	–	O6	1.871(4)
Te1	–	O9	1.968(4)
Te1	–	O3	2.480(5)
Te2	–	O4	1.864(4)
Te2	–	O8	1.864(4)
Te2	–	O9	2.058(5)
Te2	–	O2	2.335(5)
Te3	–	O3	1.869(5)
Te3	–	O2	1.884(4)
Te3	–	O7	1.926(4)

Cd1 1.96; Cd2 2.15; Cd3 1.75; Se1 5.99; Se2 6.16; Te1 3.99; Te2 3.90; Te3 3.77; O1 (Se, Cd) 1.74; O2 (2Te, Cd) 2.00; O3 (2Te, Cd) 1.97; O4 (Te, 3Cd) 2.28; O5 (Te, 3Cd) 2.19; O6 (Te, 2Cd) 2.08; O7 (Te, 3Cd) 2.07; O8 (Te, 3Cd) 2.31; O9 (2Te, Cd) 2.14; O10 (Se, Cd) 1.67; O11 (Se) 1.62; O12 (Se) 1.63; O13 (Se) 1.47; O14 (Se) 1.61

Cd$_3$(H$_2$O)(SO$_4$)(Te$_3$O$_8$)[b)]			
Cd1	–	O8	2.183(13)
Cd1	–	O6	2.329(12)
Cd1	–	O2	2.333(13)
Cd1	–	O5	2.382(12)
Cd1	–	O5	2.403(12)
Cd1	–	O9	2.482(13)
Cd1	–	O3	2.534(13)
Cd2	–	O3	2.215(13)
Cd2	–	O5	2.234(13)
Cd2	–	O2	2.322(13)
Cd2	–	O4	2.322(13)
Cd2	–	O11A	2.35(3)
Cd2	–	O2	2.471(13)
Cd2	–	O7	2.533(13)
Cd3	–	O11B	2.15(2)
Cd3	–	O11A	2.26(2)
Cd3	–	O1	2.327(12)
Cd3	–	O4	2.377(13)
Cd3	–	O3	2.406(13)
Cd3	–	O4	2.428(12)
Cd3	–	O8	2.429(13)
Cd3	–	O10	2.502(13)
S1	–	O9	1.465(14)
S1	–	O13B	1.472(10)
S1	–	O12B	1.476(9)
S1	–	O12A	1.483(10)
S1	–	O13A	1.486(9)
S1	–	O7	1.487(13)
Te1	–	O4	1.861(13)
Te1	–	O8	1.868(13)
Te1	–	O1	1.910(13)
Te2	–	O3	1.859(13)
Te2	–	O5	1.868(13)
Te2	–	O6	2.107(13)
Te2	–	O1	2.125(12)
Te3	–	O11B	1.83(2)
Te3	–	O2	1.876(13)
Te3	–	O6	1.911(13)
Te3	–	O11A	1.93(3)
O10	···	O12A	2.62(3)
O10	···	O13B	2.62(3)
O10	···	O12A	2.62(2)
O10	···	O10	2.76(3)

Cd1 2.03; Cd2 2.04; Cd3 1.98; S1 5.22; Te1 3.91; Te2 4.09; Te3 3.82; O1 (2Te, Cd) 2.19; O2 (Te, 3Cd) 2.17; O3 (Te, 3Cd) 2.19; O4 (Te, 3Cd) 2.21; O5 (Te, 3Cd) 2.29; O6 (2Te, Cd) 2.21; O7 (S, Cd) 1.63; O8 (Te, 2Cd) 2.06; O9 (S, Cd) 1.75; O10* (Cd) 0.20; O11A (Te, Cd) 1.53; O12B (Te, Cd) 1.99; O12A (S) 1.47; O12B (S) 1.49; O13A (S) 1.45; O13B(S) 1.51

a) Coordination of a specific O atoms to the type and number of chalcogen or metal atoms is indicated in parentheses. b) * Hydrogen atoms not considered for calculation of bond valence sums.

(Ca1–Ca3), respectively, sharing corners and edges. In this way a layered arrangement parallel (001) at $z \approx 0$ and ½ for the centrosymmetric Ca structure and parallel (100) at $y \approx$ ¼ and ¾ for the non-centrosymmetric Cd structure is established. The three independent Te^{IV} atoms flank the metal-oxygen layers above and below the layer planes and are connected to the outer oxygen atoms in form of TeO$_3$ trigonal pyramids (Ca structure Te2, Te3; Cd structure Te1)

Table 5. Selected interatomic distances /Å, angles /°, and bond valence sums /v.u.[a)]

$Cd_4(SO_4)(TeO_3)_3$			
Cd1	–	O8	2.208(2) 2x
Cd1	–	O13	2.296(2) 2x
Cd1	–	O7	2.330(2) 2x
Cd2	–	O9	2.272(2) 2x
Cd2	–	O5	2.273(2) 2x
Cd2	–	O6	2.375(2) 2x
Cd3	–	O2	2.196(2)
Cd3	–	O12	2.232(2)
Cd3	–	O8	2.293(2)
Cd3	–	O11	2.319(2)
Cd3	–	O3	2.393(2)
Cd3	–	O10	2.470(2)
Cd4	–	O7	2.241(2)
Cd4	–	O6	2.257(2)
Cd4	–	O9	2.290(2)
Cd4	–	O3	2.365(2)
Cd4	–	O2	2.407(2)
Cd4	–	O5	2.431(2)
Cd5	–	O1	2.292(2)
Cd5	–	O4	2.292(2)
Cd5	–	O3	2.327(2)
Cd5	–	O1	2.368(2)
Cd5	–	O4	2.399(2)
Cd5	–	O2	2.450(2)
Cd5	–	O6	2.482(2)
S1	–	O10	1.474(2)
S1	–	O11	1.474(2)
S1	–	O12	1.479(2)
S1	–	O13	1.487(2)
Te1	–	O1	1.868(2)
Te1	–	O2	1.875(2)
Te1	–	O3	1.904(2)
Te2	–	O4	1.855(2)
Te2	–	O5	1.887(2)
Te2	–	O6	1.913(2)
Te3	–	O7	1.857(2)
Te3	–	O8	1.875(2)
Te3	–	O9	1.883(2)

Cd1 2.20; Cd2 2.04; Cd3 2.02; Cd4 1.93; Cd5 2.00; S1 5.93; Te1 3.88; Te2 3.86; Te3 3.97; O1 (Te, 2Cd) 1.98; O2 (Te, 3Cd) 2.26; O3 (Te, 3 Cd) 2.09; 2Cd) 1.87; O6 (Te, 3Cd) O4 (Te, 2Cd) 2.01; O5 (Te, 2.06; O7 (Te, 2Cd) 2.10; O8 (Te, 2Cd) 2.11; O9 (Te, 2Cd) 2.01; O10 (S, Cd) 1.72; O11 (S, Cd); 1.83; O12 (S, Cd) 1.89; O13 (S, Cd) 1.80

$Cd_5(SO_4)_2(TeO_3)_2(OH)_2$			
Cd1	–	O8	2.2293(11)
Cd1	–	O4	2.2544(11)
Cd1	–	O5	2.2941(13)
Cd1	–	O3	2.3376(11)
Cd1	–	O7	2.3557(12)
Cd1	–	O2	2.3648(12)
Cd2	–	O4	2.2447(11) 2x
Cd2	–	O1	2.2813(12) 2x
Cd2	–	O6	2.4035(12) 2x
Cd3	–	O4	2.2071(11)
Cd3	–	O1	2.3057(11)
Cd3	–	O3	2.3152(11)
Cd3	–	O8	2.3622(11)
Cd3	–	O8	2.4111(12)
Cd3	–	O3	2.4414(12)
S1	–	O5	1.4665(13)
S1	–	O2	1.4678(13)
S1	–	O7	1.4774(11)
S1	–	O6	1.4887(12)
Te1	–	O1	1.8658(11)
Te1	–	O3	1.8723(11)
Te1	–	O8	1.8900(11)

D–H···*A*	D···A (*D*–H···*A*)
O4–H1···O5	2.918 145

Cd1 2.04; Cd2 2.04; Cd3 1.99; S1 5.98; Te1 3.94; O1 (Te, 2Cd) 2.05; O2 (S, Cd) 1.82; O3 (Te, 3 Cd) 2.20; O4* (3 Cd) 1.23; O5 (S, Cd) 1.88; O6 (S, Cd) 1.70; O7 (S, Cd) 1.78; O8 (Te, 3 Cd) 2.22

$Sr_3(H_2O)_2(SeO_4)(TeO_3)_2$[b)]							
Sr1	–	O11	2.443(5)	Se1	–	O13	1.577(8)
Sr1	–	O9	2.511(5)	Se1	–	O14	1.708(6)
Sr1	–	O5	2.524(5)	Se1	–	O15	1.708(6)
Sr1	–	O2	2.539(5)	Se1	–	O16	1.726(5)
Sr1	–	O20	2.571(5)	Se2	–	O18	1.635(5)
Sr1	–	O2W	2.660(6)	Se2	–	O17	1.637(6)
Sr1	–	O1W	2.687(6)	Se2	–	O19	1.643(5)
Sr2	–	O3	2.480(5)	Se2	–	O20	1.648(5)
Sr2	–	O6	2.484(5)	Te1	–	O1	1.849(6)
Sr2	–	O12	2.539(5)	Te1	–	O3	1.866(5)
Sr2	–	O8	2.545(6)	Te1	–	O2	1.867(5)
Sr2	–	O16	2.581(5)	Te2	–	O4	1.848(5)
Sr2	–	O3W	2.660(6)	Te2	–	O5	1.862(4)
Sr2	–	O4W	2.791(7)	Te2	–	O6	1.875(5)
Sr2	–	O1	3.201(6)	Te3	–	O7	1.833(7)
Sr3	–	O2	2.565(5)	Te3	–	O8	1.851(5)
Sr3	–	O5	2.587(5)	Te3	–	O9	1.865(5)
Sr3	–	O6	2.653(5)	Te4	–	O10	1.833(5)
Sr3	–	O9	2.653(5)	Te4	–	O11	1.839(5)
Sr3	–	O5	2.670(5)	Te4	–	O12	1.857(5)
Sr3	–	O8	2.688(6)				
Sr3	–	O14	2.722(6)	O1W	···	O17	2.864(9)
Sr3	–	O1	3.269(6)	O1W	···	O16	2.873(8)
Sr4	–	O10	2.447(5)	O1W	···	O9	3.164(8)
Sr4	–	O1	2.478(5)	O1W	···	O20	3.230(8)
Sr4	–	O8	2.556(6)	O2W	···	O18	2.864(9)
Sr4	–	O12	2.578(5)	O2W	···	O16	2.877(8)
Sr4	–	O19	2.600(6)	O2W	···	O20	3.158(8)
Sr4	–	O15	2.659(6)	O2W	···	O2	3.169(8)
Sr4	–	O19	2.743(6)	O3W	···	O20	2.915(8)
Sr5	–	O7	2.440(6)	O3W	···	O15	2.931(11)
Sr5	–	O4	2.467(5)	O3W	···	O16	3.133(9)
Sr5	–	O10	2.509(6)	O3W	···	O3	3.242(11)
Sr5	–	O14	2.633(6)	O4W	···	O13	2.759(12)
Sr5	–	O9	2.637(5)	O4W	···	O20	3.036(9)
Sr5	–	O7	2.725(7)	O4W	···	O8	3.090(9)
Sr5	–	O17	2.773(6)	O4W	···	O16	3.258(9)
Sr5	–	O13	2.825(8)				
Sr5	–	O11	3.057(7)				
Sr6	–	O4	2.556(5)				
Sr6	–	O3	2.608(5)				
Sr6	–	O18	2.638(6)				
Sr6	–	O2	2.678(5)				
Sr6	–	O12	2.721(6)				
Sr6	–	O3	2.733(5)				
Sr6	–	O1	2.768(6)				
Sr6	–	O11	2.862(6)				
Sr6	–	O6	2.925(6)				

Sr1 2.16; Sr2 2.06; Sr3 1.69; Sr4 2.07; Sr5 1.84; 2.16; Sr6 1.84; Se1 5.45; Se2 5.96; Te1 4.11; Te2 4.10; Te3 4.23; Te4 4.37; O1 (Te, 2Sr) 1.96; O2 (Te, 3Sr) 2.18; O3 (Te, 3Sr) 2.18; O4 (Te,2Sr) 2.11; O5 (Te, 3Sr) 2.21; O6 (Te, 3Sr) 2.04; O7 (Te, 2Sr) 2.09; O8 (Te, 3 Sr) 2.24; O9 (Te, 3Sr) 2.18; O10 (Te, 2Sr) 2.23; O11(Te, 2Sr) 2.00; O12 (Te, 3Sr) 1.93; O13 (Se, Sr) 1.92; O14 (Se, 2Sr) 1.69; O15 (Se, Sr) 1.47; O16 (Se, Sr) 1.47; O17 (Se, Sr) 1.67; O18 (Se, Sr) 1.76; O19 (Se, 2Sr) 1.94; O20 (Se, Sr) 1.75; O1W* (Sr) 0.22; O2W* (Sr) 0.23; O3W* (Sr) 0.23; O4W* (Sr) 0.16

a) Coordination of a specific O atoms to the type and number of chalcogen or metal atoms is indicated in parentheses. b) * Hydrogen atoms not considered for calculation of bond valence sums.

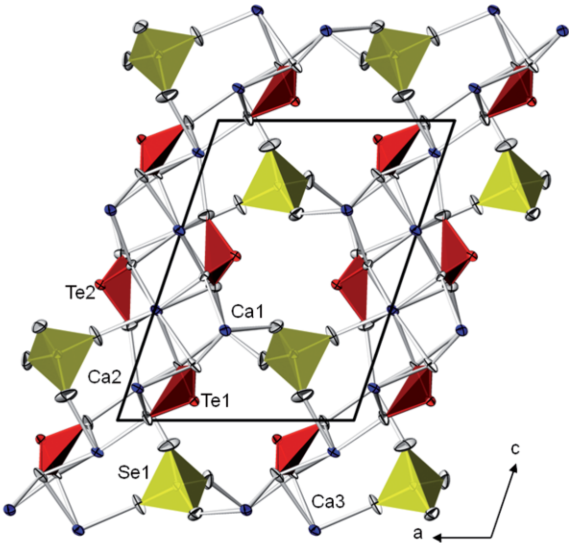

Figure 1. The crystal structure of $Ca_3(SeO_4)(TeO_3)_2$ in a projection along [010]. Te atoms and corresponding polyhedra are given in red, Se atoms and corresponding polyhedra in yellow, Ca atoms in blue, O atoms are colourless. Displacement ellipsoids are drawn at the 74 % probability level.

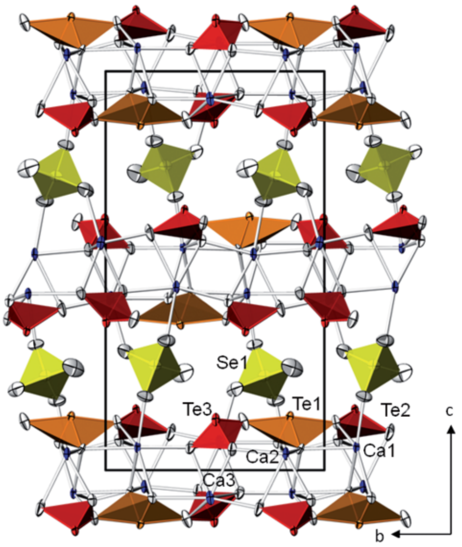

Figure 2. The crystal structure of $Ca_3(SeO_4)(Te_3O_8)$ in a projection along [100]. Te atoms with coordination number three and corresponding polyhedra are given in red, Te atoms with coordination number four and corresponding polyhedra are given in orange. Se atoms and corresponding polyhedra, Ca atoms, O atoms as well as displacement ellipsoids are as in Figure 1.

and TeO_4 disphenoids (Ca structure Te1; Cd structure Te1, Te2). In both structures the electron lone pairs of the Te^{IV} atoms are pointing away from the metal-oxygen layer. The connectivity of the TeO_3 and TeO_4 polyhedra is markedly different in the two structures. Whereas finite Te_3O_8 groups $[Te2O_{2/1}O_{1/2}Te1O_{2/2}O_{2/1}Te3O_{1/2}O_{2/1}]$ or $[(TeO_{2/1}O_{1/2})_2TeO_{2/2}O_{2/1}]$ are realized in $Ca_3(SeO_4)(Te_3O_8)$, infinite zigzag chains Te_3O_8 $[Te1O_{2/1}O_{2/2}Te1O_{1/1}O_{2/2}Te3O_{2/1}O_{2/2}]^1_\infty$ are present in $Cd_3(SeO_4)(Te_3O_8)$. The connection of adjacent layers in both structures is accomplished by isolated SeO_4 tetrahedra that are relatively loosely bonded to the metal cations. In fact, some of the selenate oxygen atoms do not show any bonding with the metal cations at all, which explains their rather low bond valence sums (Table 4) and their high displacement parameters (Figure 2 and Figure 3). On the other hand, these single-bonded O atoms show, as expected, the shortest Se–O distances.

$Cd_3(H_2O)(SO_4)(Te_3O_8)$

The principal structural set-up of this hydrous phase (Figure 4) is very similar to that of the two $M_3(SeO_4)(Te_3O_8)$ phases, i.e. a layered arrangement of metal–oxygen (M = Cd) and tellurium–oxygen polyhedra sandwiched by XO_4 tetrahedra (X = Se, S). The three cadmium cations exhibit coordination numbers of seven (Cd1, Cd3) and of six or seven (Cd2), taking into account the half-occupancy of an oxygen atom (O11A) that is part of the coordination sphere of the latter cation. The corresponding CdO_x (x = 6, 7) polyhedra are distorted and condensed into a layered arrangement through corner- and edge-sharing. The layers spread parallel to (001) at $z \approx 0$. Again, the Te^{IV} atoms flank the layers above and below the outer oxygen atoms of the layers, forming two TeO_3 trigonal pyramids (Te1, Te3) and a TeO_4 bisphenoid (Te2) with the electron lone pair pointing away from the layer. The anion has the same finite Te_3O_8 configuration than that in $Ca_3(SeO_4)(Te_3O_8)$ ($[(TeO_{2/1}O_{1/2})_2TeO_{2/2}O_{2/1}]$). In comparison with the latter structure, an additional water molecule (O10) is bonded to one of the Cd atoms (Cd3) and is positioned between two layers. Although the hydrogen atoms of the water molecule could not be located in the present study, bond valence sums and typical O···O donor···acceptor distances (Table 4) clearly support the presence of O10 as part of a water molecule that is involved in hydrogen bonding of medium strengths (O10···O(acceptor) distances 2.62–2.76 Å).

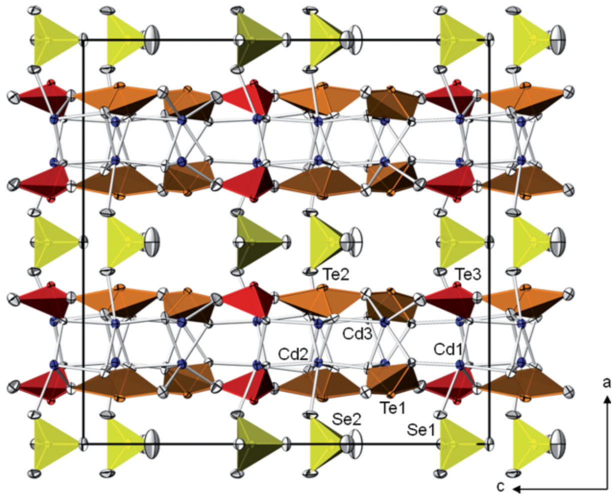

Figure 3. The crystal structure of $Cd_3(SeO_4)(Te_3O_8)$ in a projection along [010]. Cd atoms are blue, all other atoms, polyhedra and ellipsoids are drawn as in Figure 2.

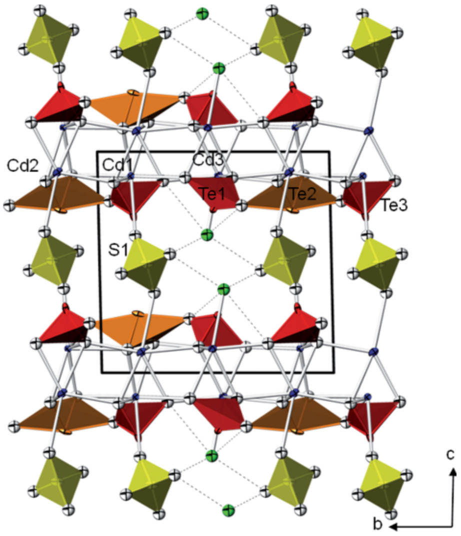

Figure 4. The crystal structure of $Cd_3(H_2O)(SO_4)(Te_3O_8)$ in a projection along [100]. O atoms belonging to the OH group are green, all other atoms, polyhedra and ellipsoids are drawn as in Figure 3. Possible hydrogen-bonding interactions are depicted as dashed lines. Only one of the orientations of the disordered O atoms is shown.

The sulfate tetrahedra are disordered over two sets of sites and are situated at $z \approx ½$ between the cadmium oxotellurate(IV) layers. The SO_4 anions alternate pairwise with the water molecule along [010]. A notable difference between the $M_3(SeO_4)$-(Te_3O_8) and the $Cd_3(H_2O)(SO_4)(Te_3O_8)$ structure pertains to the distance between two layers. The interlayer gap, measured as the shortest distance between the most outer oxygen atoms of adjacent layers, is 3.44 Å in $Ca_3(SeO_4)(Te_3O_8)$, 3.95 Å in $Cd_3(SeO_4)(Te_3O_8)$, and 4.26 Å in $Cd_3(H_2O)(SO_4)(Te_3O_8)$. Although the SO_4 tetrahedron is smaller than the SeO_4 tetrahedron, the interlayer gap is the longest for the sulfate compound and hence might explain the disorder of the SO_4 anion with its O atoms bound either loosely to the cadmium atoms of the layer or hydrogen-bonded to the water molecule.

$Cd_4(SO_4)(TeO_3)_3$

In contrast to the distinct layered arrangements of the $Ca_3(SeO_4)(Te_3O_8)$, $Cd_3(SeO_4)(Te_3O_8)$, and $Cd_3(H_2O)(SeO_4)$-(Te_3O_8) structures, each of which is also characterized by the presence of condensed oxotellurate anions $[Te_3O_8]^{4-}$, the structure of $Cd_4(SO_4)(TeO_3)_3$ represents a three-dimensional framework of individual building blocks, whereby the tellurate anions are not condensed with each other (Figure 5). Five unique Cd^{2+} cations are present in the asymmetric unit, two (Cd1, Cd2) located on a centre of inversion. Except Cd5 with a distorted monocapped octahedral coordination by O atoms, all other Cd cations exhibit distorted octahedral coordination spheres, most prominently pronounced for Cd4. The various CdO_x polyhedra share O atoms through vertices and edges, thereby constructing a three-dimensional framework. The latter is crossed by channels parallel to [100] where the three independent Te atoms are located. Again, the stereochemical activity of the Te^{IV} atoms is evident from the direction of the electron lone pairs towards the empty space of the channels. As noted above, $Cd_4(SO_4)(TeO_3)_3$ does not contain condensed oxotellurate anions but isolated trigonal-pyramidal TeO_3 groups only. The S atoms of the slightly distorted sulfate tetrahedra are arranged in layers parallel to (002). A remarkable difference to the $Ca_3(SeO_4)(Te_3O_8)$, $Cd_3(SeO_4)(Te_3O_8)$, and $Cd_3(H_2O)(SeO_4)(Te_3O_8)$ structures is the coordination of *all* sulfate O atoms to a Cd^{2+} cation.

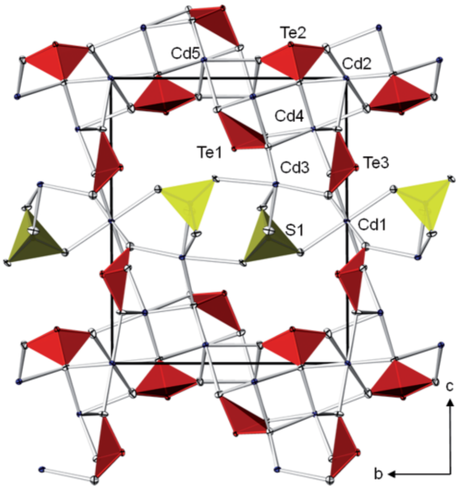

Figure 5. The crystal structure of $Cd_4(SO_4)(TeO_3)_3$ in a projection along [100]. S atoms and SO_4 polyhedra are yellow, all other atoms, polyhedra and ellipsoids are drawn as in Figure 3.

$Cd_5(SO_4)_2(TeO_3)_2(OH)_2$

Although the crystal structure of $Cd_5(SO_4)_2(TeO_3)_2(OH)_2$ (Figure 6) is likewise built up from metal oxotellurate(IV) layers, it shows resemblance to the framework structure of $Cd_4(SO_4)(TeO_3)_3$ rather than to the three layered structures

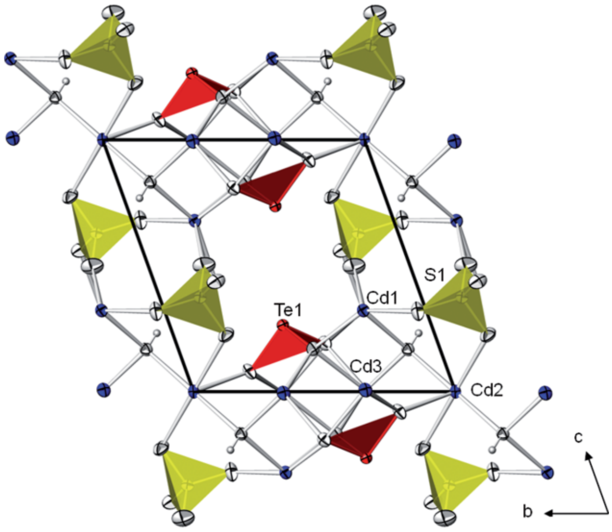

Figure 6. The crystal structure of $Cd_5(SO_4)_2(TeO_3)_2(OH)_2$ in a projection along [100]. Hydrogen atoms are represented as grey spheres with an arbitrary radius; colour codes for other atoms and polyhedra, as well as the probability function of the ellipsoids are as in Figure 5.

discussed above. All three independent Cd^{2+} cations in $Cd_5(SO_4)_2(TeO_3)_2(OH)_2$ (Cd2 with site symmetry $\bar{1}$) are surrounded by six O atoms in the form of distorted octahedra. Cd2 and Cd3 are situated at $z \approx 0$ and are condensed through common O atom vertices and edges into layers parallel to (001). The Cd1 cations flank these layers in an alternating up and down mode at $z \approx 1/3$ and $z \approx -1/3$. Adjacent layers are held together by sulfate tetrahedra, here again with *all* sulfate O atoms additionally bonded to a Cd^{2+} cation. This arrangement delimits channels propagating parallel to [100] into which the electron lone pairs of the Te^{IV} atoms of the isolated $Te1O_3$ trigonal pyramids protrude. Additional stabilization of this arrangement is achieved through a weak hydrogen bonding interaction between the OH group (O4) and one of the sulfate O atoms (O4···O5 2.918 Å; Table 5, Figure 6).

$Sr_3(H_2O)_2(SeO_4)(TeO_3)_2$

Six Sr cations, four with a coordination number of seven (Sr1–Sr4) and two with coordination number eight (Sr5–6) are present in the asymmetric unit. The crystal structure of this phase is depicted in Figure 7. Cations Sr3–Sr6 are situated at $x \approx 0$ and build up strontium-oxygen sheets parallel (100) with the remaining two Sr1 and Sr2 cations located on both sides of the sheets. Next to the O atoms that are part of the strontium-oxygen sheet, these two cations each are additionally bonded to two water molecules directed towards the neighbouring sheet. Besides rather weak possible inter-sheet hydrogen bonds between the water molecules and O atoms of adjacent sheets (OW···O distance between 3.1 and 3.2 Å), the connection between the sheets is mainly accomplished through bridging SeO_4 tetrahedra along [100]. Atom Se1 shows a disparate Se–O bond lengths distribution with one short and three longer bonds, whereas Se2 is more uniformly structured with more or less the same bond lengths. Three O atoms of each independent SeO_4 tetrahedron are also involved as acceptor atoms for hydrogen-bonding with the water molecules, here with significant shorter OW···O distances compared to the inter-sheet interactions, ranging from 2.75–3.1 Å. The role as hydrogen-bonding acceptor atoms also compensates for the considerable underbonding of these atoms (Table 5), which, next to their features as selenate oxygen atoms, are bonded only at large distances to the Sr^{2+} ions of the sheets. Like in all other structures presented in this communication, the arrangement of the metal–oxygen sheets and the tetrahedral oxochalcogenate(VI) units leads to the formation of free space, in this case associated with channels running parallel to [001]. Here the four unique Te atoms are located at the outer array of the sheets, alternating with the Se atoms along [010] on each side of the sheet. The motif of trigonal-pyramidal TeO_3 units pointing with their electron lone pairs into the empty space of the channels is also found in the structure of $Sr_3(H_2O)_2(SeO_4)(TeO_3)_2$.

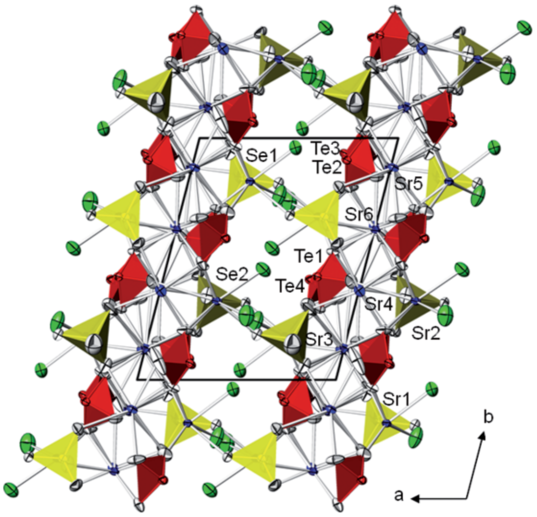

Figure 7. The crystal structure of $Sr_3(H_2O)_2(SeO_4)(TeO_3)_2$ in a projection along [001]. Sr atoms are blue, O atoms belonging to water molecules are green. Colour codes for other atoms and polyhedra, as well as the probability function of the ellipsoids are as in Figure 1.

General Features

In all seven crystal structures, the oxochalcogenate(VI) anions are isolated from the oxotellurate(IV) anions and show bond lengths distributions characteristic for tetrahedral XO_4 (X = S, Se) groups.[51,52] The same applies for the respective metal–oxygen polyhedra[53–55] with coordination numbers ranging between six and eight for Ca^{2+}, six and seven for Cd^{2+} and seven and eight for Sr^{2+} compounds, in accordance with the increasing ionic radii from Cd to Sr.[56]

Conclusions

The idea to modify metal oxotellurate(IV) frameworks (metal = Ca, Cd, Sr) through incorporation of tetrahedral XO_4 anions (X = S, Se) as spacers with formation of compounds with non-centrosymmetric structures has proven to be successful for two out of seven new compounds. Corresponding reaction batches were conducted under hydrothermal conditions and led to multi-phase mixtures with low yields for the mixed oxochalcogenate(IV,VI) phases in each case. $Ca_3(SeO_4)$-$(TeO_3)_2$ and $Cd_3(SeO_4)(Te_3O_8)$ crystallize in space group types $P2_1$ and $Cmc2_1$, respectively, whereas $Ca_3(SeO_4)(Te_3O_8)$ ($P2_1/n$), $Cd_3(H_2O)(SO_4)(Te_3O_8)$, $Cd_4(SO_4)(TeO_3)_3$, $Cd_5(SO_4)_2(TeO_3)_2(OH)_2$, and $Sr_3(H_2O)_2(SeO_4)(TeO_3)_2$ (all $P\bar{1}$) crystallize in centrosymmetric space group types. Common to all crystal structures are the stereoactivity of the Te $5s^2$ electron lone pair E and the separation of the tetrahedral $XO_4{}^{2-}$ anions and oxotellurate anions, the latter being present either as single $TeO_3{}^{2-}$ anions or as condensed $[Te_3O_8]^{4-}$ anions. Low yields and multi-phase formation prevented further examination of physical properties of the title compounds.

Acknowledgements

The X-ray Centre of TU Wien is acknowledged for providing access to the single-crystal and powder diffractometers.

Keywords: Crystal engineering; Hydrothermal synthesis; Oxotellurates(IV); Mixed oxochalcogenates; Crystal structure

References

[1] A. G. Christy, S. J. Mills, A. R. Kampf, *Mineral. Mag.* **2016**, *80*, 415–545.
[2] J. Galy, J. Meunier, S. Andersson, A. Åström, *J. Solid State Chem.* **1975**, *13*, 142–159.
[3] J. Zemann, *Monatsh. Chem.* **1971**, *102*, 1209–1216.
[4] M. Trömel, *J. Solid State Chem.* **1980**, *35*, 90–98.
[5] V. A. Dolgikh, *Russ. J. Inorg. Chem.* **1991**, *36*, 1117–1129.
[6] A. V. Marukhnov, D. V. Pushkin, V. N. Serezhkin, *Russ. J. Inorg. Chem.* **2007**, *52*, 203–208.
[7] R. Rai, S. Sharma, R. N. P. Choudhary, *J. Mater. Sci. Lett.* **2002**, *21*, 297–299.
[8] T. Yamada, *Rev. Electr. Commun. Lab.* **1975**, *23*, 564–568.
[9] T. Yamada, H. Iwasaki, *Appl. Phys. Lett.* **1972**, *21*, 89–90.
[10] V. E. Zavodnik, S. A. Ivanov, A. I. Stash, *Acta Crystallogr., Sect. E* **2007**, *63*, i52.
[11] V. E. Zavodnik, S. A. Ivanov, A. I. Stash, *Acta Crystallogr., Sect. E* **2007**, *63*, i75–i76.
[12] V. E. Zavodnik, S. A. Ivanov, A. I. Stash, *Acta Crystallogr., Sect. E* **2007**, *63*, i151.
[13] V. E. Zavodnik, S. A. Ivanov, A. I. Stash, *Acta Crystallogr., Sect. E* **2007**, *63*, i111–i112.
[14] B. Stöger, M. Weil, E. J. Baran, A. C. Gonzáles-Baró, S. Malo, J. M. Rueff, S. Petit, M. B. Lepetit, B. Raveau, N. Barrier, *Dalton Trans.* **2011**, *40*, 5538–5548.
[15] B. Stöger, M. Weil, G. Giester, *Acta Crystallogr., Sect. B* **2009**, *65*, 167–181.
[16] M. Poupon, N. Barrier, S. Petit, S. Clevers, V. Dupray V, *Inorg. Chem.* **2015**, *54*, 5660–5670.
[17] M. Weil, M. Shirkhanlou, *Z. Anorg. Allg. Chem.* **2015**, *641*, 1459–1466.
[18] A. Rabenau, *Angew. Chem.* **1987**, *99*, 1017–1032.
[19] G. B. Johansson, O. Lindqvist, *Acta Crystallogr., Sect. B* **1976**, *32*, 407–411.
[20] F. Pertlik, *Tschermaks Mineral. Petrogr. Mitt.* **1971**, *15*, 279–290.
[21] F. Pertlik, J. Zemann, *Monatsh. Chem.* **1988**, *119*, 311–317.
[22] F. Pertlik, J. Zemann, *Mineral. Petrol.* **1988**, *38*, 291–298.
[23] J. Lin, P. Chai, K. Diefenbach, M. Shatruk, T. E. Albrecht-Schmitt, *Chem. Mater.* **2014**, *26*, 2187–2194.
[24] J. Lin, K. Diefenbach, M. A. Silver, N. S. Dalal, T. E. Albrecht-Schmitt, *Cryst. Growth Des.* **2015**, *15*, 4606–4615.
[25] J. Lin, J. N. Cross, J. Diwu, N. A. Meredith, T. E. Albrecht-Schmitt, *Inorg. Chem.* **2013**, *52*, 4277–4281.
[26] Y.-Y. Tang, Z.-Z. He, W.-B. Guo, S.-Y. Zhang, M. Yang, *Inorg. Chem.* **2014**, *53*, 5862–5868.
[27] F.-T. Chen, J.-C. Zhao, J.-L. Xu, Y.-D. Wu, *Z. Anorg. Allg. Chem.* **2015**, *641*, 568–572.
[28] S. Y. Song, D. W. Lee, K. M. Ok, *Inorg. Chem.* **2014**, *53*, 7040–7046.
[29] E. P. Lee, S. Y. Song, D. W. Lee, K. M. Ok, *Inorg. Chem.* **2013**, *52*, 4097–4103.
[30] O. Lindqvist, *Acta Chem. Scand.* **1968**, *22*, 977–982.
[31] D. Hottentot, B. O. Loopstra, *Acta Crystallogr., Sect. B* **1979**, *35*, 728–729.
[32] H. Effenberger, J. Zemann, H. Mayer, *Am. Mineral.* **1978**, *63*, 847–852.
[33] M. J. Redman, J. H. Chen, W. P. Binnie, W. J. Mallio, *J. Am. Ceram. Soc.* **1970**, *53*, 645–648.
[34] a) M. Weil, B. Stöger, *Acta Crystallogr., Sect. C* **2008**, *64*, i79-i81; b) N. Barrier, J. M. Rueff, M. B. Lepetit, J. Contreras-Garcia, S. Malo, B. Raveau, *Solid State Sci.* **2009**, *11*, 289–293.
[35] M. Weil, *Solid State Sci.* **2004**, *6*, 29–37.
[36] V. Krämer, G. Brandt, *Acta Crystallogr., Sect. C* **1985**, *41*, 1152–1154.
[37] G. Bertrand, Y. Dusausoy, *C. R. Seances Acad. Sci. Ser. C* **1970**, *270*, 612–615.
[38] M. E. Straumanis, P. M. Vora, A. A. Khan, *Z. Anorg. Allg. Chem.* **1971**, *383*, 211–219.
[39] H. G. Burckhardt, C. Platte, M. Trömel, *Acta Crystallogr., Sect. B* **1982**, *38*, 2450–2452.
[40] M. Weil, M. Shirkhanlou, *Acta Crystallogr., Sect. E* **2016**, *72*, 1532–1535.
[41] SMART, APEX-2, SAINT, SADABS, TWINABS and RLATT. Bruker AXS Inc., Madison, Wisconsin, USA.
[42] G. M. Sheldrick, *Acta Crystallogr., Sect. A* **2008**, *64*, 112–122.
[43] I. D. Brown. *The Chemical Bond in Inorganic Chemistry: The Bond Valence Model*. Oxford University Press, Oxford, England, **2002**.
[44] N. E. Brese, M. O'Keeffe, *Acta Crystallogr., Sect. B* **1991**, *47*, 192.
[45] E. Dowty, ATOMS for Windows (version 6.3). Shape Software, 521 Hidden Valley Road, Kingsport, TN 37663 (USA).
[46] D. K. Breitinger, in *Comprehensive Coordination Chemistry II* (Eds.: J. A. McCleverty, T. J. Meyer), ch. 6, pp. 1253–1292, Elsevier, Oxford, **2004**.
[47] E. R. Losilla, M. A. G. Aranda, F. J. Ramirez, S. Bruque, *J. Phys. Chem.* **1995**, *99*, 12975–12979.
[48] a) M. Weil, *Z. Naturforsch.* **2000**, *55b*, 699–706; b) T. J. Mormann, W. Jeitschko, *Z. Kristallogr. NCS* **2000**, *215*, 471–472.
[49] G. de la Flor, D. Orobengoa, E. Tasci, J. M. Perez-Mato, M. I. Aroyo, *J. Appl. Crystallogr.* **2016**, *49*, 653–664.
[50] G. Bergerhoff, M. Berndt, K. Brandenburg, T. Degen, *Acta Crystallogr., Sect. B* **1999**, *55*, 147–156.
[51] F. C. Hawthorne, S. V. Krivovichev, P. C. Burns, *Rev. Mineral. Geochem.* **2000**, *40*, 1–112.
[52] M. S. Wickleder, C. Logemann: Compounds Containing the Chalcogen Oxygen *E*–O, Bond (*E* = S, Se, Te), in: *Handbook on Chalcogen Chemistry*, 2nd edition (ed. F. Devillanova), Royal Society of Chemistry, London, **2013**.
[53] G. Chiari, G. Ferraris, *Z. Kristallogr.* **1990**, *191*, 39–43.
[54] V. A. Blatov, L. V. Pogildyakova, V. N. Serezhkin, *Acta Crystallogr., Sect. B* **1999**, *55*, 139–146.
[55] O. C. Gagné, F. C. Hawthorne, *Acta Crystallogr., Sect. B* **2016**, *72*, 602–625.
[56] R. D. Shannon, *Acta Crystallogr., Sect. A* **1976**, *22*, 551–767.

Received: October 28, 2016

M. Weil, M. Shirkhanlou* **1–11**

Incorporation of Sulfate or Selenate Groups into Oxotellurates(IV): I. Calcium, Cadmium, and Strontium Compounds